A&A 369, 971–980 (2001)
DOI: 10.1051/0004-6361:20010173

Astronomy & Astrophysics

X-ray emission of multiple T Tauri stars in Taurus

B. König[1], R. Neuhäuser[1,2], and B. Stelzer[1]

[1] MPI für extraterrestrische Physik, Giessenbachstraße 1, 85740 Garching, Germany
[2] Institute for Astronomy, University of Hawaii, Honolulu, USA

Received 29 February 2000 / Accepted 26 January 2001

Abstract. We present a study of X-ray emission of known multiple T Tauri stars (TTS) in Taurus based on ROSAT observations. We used the ROSAT All-Sky Survey (RASS) detection rates of single classical (cTTS) and weak-line TTS (wTTS) to investigate statistically the TTS nature (classical or weak-line) of the components in multiple TTS, which are too close for spatially resolved spectroscopy so far. Because single wTTS show a higher RASS detection rate than single cTTS, the different binary TTS (cTTS-cTTS, cTTS-wTTS, wTTS-wTTS) should also have different detection rates. We find that the observed RASS detection rates of binary wTTS, where the nature of the secondary is unknown, are in agreement with the secondaries being wTTS rather than cTTS, and mixed pairs are very rare. Furthermore we analyse the X-ray emission of TTS systems resolvable by the ROSAT HRI. Among those systems we find statistical evidence that primaries show larger X-ray luminosity than secondaries, and that the samples of primary and secondary TTS are similar concerning the X-ray over bolometric luminosity ratios. Furthermore, primaries always emit harder X-rays than secondaries. In all cases where rotational velocities and/or periods are known for both companions, it is always the primary that rotates faster. Hence, the stronger X-ray emission of the primaries may be due to higher bolometric luminosity and/or faster rotation.

Key words. stars: formation – late-type – low-mass

1. Introduction

Late type pre-main sequence stars (PMS) are well-established as X-ray emitters. The soft X-rays are believed to be generated in a hot optically thin coronal plasma at temperatures above 10^6 K (Feigelson & DeCampli 1981). The heating process is most likely related to dynamo generated magnetic fields and often described in analogy to the solar case. Indications for the connection between X-ray emission of late-type stars and dynamo activity are e.g. the observed correlations between rotation rate and X-ray luminosity. Whether such correlations hold for PMS stars is still disputed (e.g. Bouvier 1990; Neuhäuser et al. 1995b (hereafter N95) and Stelzer & Neuhäuser 2000 find such a correlation while Gagné et al. 1995 do not confirm it). For a recent review of X-ray emission from TTS see Feigelson & Montmerle (1999).

N95 have shown that in the Taurus region weak-line T Tauri stars (wTTS), i.e. TTS with weak H_α-emission and no obvious signs of accretion, are more X-ray luminous than classical T Tauri stars (cTTS). Stelzer & Neuhäuser (2000) have ruled out an X-ray selection bias, the mass distribution and a direct relation to the age of the stars as possible reasons for this discrepancy. The differences, however, may be an indirect age effect related to the different stages of the rotational evolution of cTTS and wTTS: wTTS having lost their circumstellar disk should spin up, and if the rotation rate governs the level of X-ray emission (as expected from the dynamo model) show stronger X-ray emission than cTTS. Feigelson et al. (1993) and Grosso et al. (2000) have studied the Chameleon I and the ρ Ophiuchi star formation regions, respectively, and have found that cTTS and wTTS are coeval in these regions and show similar levels of X-ray emission.

In the Taurus star-forming region the frequency of multiple stars seems to be higher than in the field (Leinert et al. 1993; Ghez et al. 1993; Köhler & Leinert 1998). Therefore this region is well suited for a study of the different aspects of X-ray emission from TTS multiples. In this paper we focus on two issues: (A) The TTS nature if the components in multiple systems, i.e. their cTTS or wTTS character, and (B) the influence of rotation and mass on the X-ray emission of TTS.

In the optical, it is not easy to assess the nature of the components. For example in a spectra covering H_α-emission line, the much wider H_α-line of the cTTS

Send offprint requests to: B. König,
e-mail: bkoenig@mpe.mpg.de

"swallows" the H_α-line of a wTTS companion. Hence, for a cTTS binary one can not determine the nature of the companion unless one can obtain spatially resolved data. For the same reason in a wTTS binary, the secondary cannot be a cTTS, unless it is much fainter than the primary. Prato & Simon (1997) and Brandner & Zinnecker (1997) tried to uncover the nature of both components of TTS pairs by taking high resolution optical spectra of all components. They conclude that close pairs with separations $\leq 3''$ (which corresponds to about 400 AU at 140 pc, Elias 1978; Wichmann et al. 1998) often have the same nature (weak-line or classical). Hartigan et al. (1994) estimated ages for wide binaries and found that 2/3 of the pairs have identical ages within the uncertainties, independent of their separation. We obtain some information about the nature of TTS in binaries by investigating the detection rates of single and binaries TTS in the spatially complete ROSAT All-Sky Survey (RASS).

Because the RASS detection rates of single cTTS and wTTS are different in Taurus we can work out expected detection rates for binary cTTS-cTTS, cTTS-wTTS and wTTS-wTTS and compare these with the observed ones for binaries. This issue is discussed in Sect. 3.

In the second part, we investigate the details of the X-ray emission of ROSAT HRI resolvable TTS binaries (Sect. 4). Previous studies of the age-rotation-activity connection have mixed up stars with different radii, ages, masses, distances and metallicities. Since X-ray emission could depend on any of those parameters, it is difficult to assess intrinsic correlations. An ideal sample to investigate the origin of the X-ray emission would consist of stars which are similar in all but one parameter. In the absence of such a uniform sample, resolved binaries may be a good choice, because they have at least the same age, distance and metallicity. We study a sample of visual multiple TTS, to investigate whether primary and secondary are different concerning L_X, L_X/L_{bol}, spectral hardness and the influence of the rotation rate on the observed differences.

2. The ROSAT data

The X-ray telescope and the instrumentation on board the ROSAT satellite have been described by Trümper (1983), Pfeffermann et al. (1988) and David et al. (1999). Two X-ray detectors are available: the Positional Sensitive Proportional Counter (PSPC) and the High Resolution Imager (HRI). During the first month of operation ROSAT has performed an All-Sky Survey (RASS). During this survey, the PSPC scanned the whole sky in great circles of $2^\circ \times 360^\circ$. The energy resolution of the PSPC is 0.1 to 2.4 keV in 256 energy channels. The spatial resolution of the HRI is $5''$ on axis. The detector has 16 channels which cover the energy range from 0.1 keV to 2.4 keV.

3. The RASS study of detection rates

In this section we employ the RASS detection rates of single cTTS and wTTS in the Taurus region to investigate statistically the TTS nature of the components in unresolved binaries. N95 have shown that the detection rate of single cTTS is different from the detection rate of single wTTS in Taurus: wTTS are less absorbed in X-rays than cTTS, because cTTS are still surrounded by circumstellar material, and even when correcting for the individual stellar absorption, wTTS are intrinsically more X-ray luminous than cTTS.

We extend the sample by including TTS identified since N95 (see Table 1) excluding ROSAT discovered TTS to avoid a possible X-ray bias. Let x be the RASS detection rate of single cTTS. Then the expected detection rate of two cTTS forming an unresolvable binary is $1-(1-x)^2$, and analogously for wTTS. The expected detection rate of mixed binaries (cTTS-wTTS) is $1-(1-x_c)(1-x_w)$ where x_c is the detection rate of single cTTS, and x_w the detection rate of single wTTS. Hence, we can check whether the detection rate of spatially unresolved cTTS binaries is consistent with them either being cTTS-wTTS or cTTS-cTTS pairs. Analogously we check if the wTTS binary detection rate is consistent with cTTS-wTTS or wTTS-wTTS pairs.

3.1. The RASS sample of TTS and the data reduction

The sample for the RASS study consists of all known TTS (except ROSAT discovered TTS) in Taurus located in the region between $\alpha_{2000} = 2$ h and 5 h and $\delta_{2000} = 14^\circ$ and 40°. It is taken from Herbig & Bell (1988), Ghez et al. (1993), N95, Kenyon & Hartmann (1995), Torres et al. (1995), Oppenheimer et al. (1997), Mathieu et al. (1997), Ghez et al. (1997b), Briceño et al. (1998), Reid & Hawley (1999), Gizis & Reid (1999), Duchêne (1999) and Koresko (2000).

Our sample is larger than the one discussed by N95. The newly identified TTS are listed in Table 1. The RASS data of these TTS has been reduced as in N95 but with the newer Extended Scientific Analysis System (EXSAS; Zimmermann et al. 1998) version 99. The source detection and identification is based on a maximum likelihood method described by Cruddace et al. (1988). We have decided on a minimum threshold value for the maximum likelihood $ML = 7.4$ above the local background following N95. This corresponds to a probability of existence of 0.993 which corresponds to $\sim 3.5\,\sigma$. For source identification we have allowed a maximum distance between the X-ray and the optical position of $40''$ shown by N95 to produce reliable source identifications.

Due to the short exposure times during the RASS ($\sim$500 s per source) a detailed spectral analysis is not possible. Some spectral information can however be obtained from the PSPC hardness ratios:

$$HR1 = \frac{H1 + H2 - S}{H1 + H2 + S}, \quad HR2 = \frac{H2 - H1}{H1 + H2}. \tag{1}$$

where the soft band (S) covers 0.1 to 0.4 keV, the hard 1 band ($H1$) 0.5 to 0.9 keV and the hard 2 band ($H2$) 0.9 to 2.0 keV. In Table 1 we give the X-ray data derived during the RASS observations of TTS not included in N95. Listed are the designation of the star, multiplicity (b: binary) and TTS characteristics (c or w), counts or upper limit (for counts) and exposure time. The hardness ratio of the two detected TTS are: RW Aur $HR1 \geq -0.18$, $HR2 = 0.56 \pm 0.11$ and IRAS 04429+1550 $HR1 = 0.62 \pm 0.10$, $HR2 = 0.14 \pm 0.12$.

The further analysis was carried out using the sample of N95 with revised classification and show their detection status (Table 5). To this sample we add the newly discovered TTS listed in Table 1.

3.2. EO detection bias concerning binary TTS

TTS which were discovered by X-ray missions could introduce a bias towards an overrepresentation of unresolved binaries, because these are X-ray brighter than single stars. Both *Einstein Observatory* (EO) (Walter et al. 1988) and ROSAT have discovered many new wTTS (Neuhäuser et al. 1995a; Wichmann et al. 1996; Magazzu et al. 1997) in Taurus. To avoid such a bias we have excluded all ROSAT-discovered TTS: they are more widely distributed than the previously known wTTS and cTTS, so that their membership to Taurus is under dispute (for a discussion see Neuhäuser 1997). EO-discovered TTS seem to be less critical: they are mainly concentrated on the clouds, because the EO pointings were directed towards previously known on-cloud TTS. The bias introduced by the EO discovery will be discussed in the following.

As in any flux-limited survey, we expect a bias regarding unresolved binaries in samples of new TTS identified among EO or RASS sources because binaries are X-ray brighter. In this section we estimate the X-ray detection bias towards binaries discovered with the EO. In the sample of TTS not originally discovered by means of X-ray emission, 15 out of 49 binaries are detected in the RASS (see Table 5). And there are 9 RASS detections among the 25 EO discovered TTS binaries (see Table 2). This results in a detection bias for EO of 1.18 ± 0.5 which is consistent with previous estimates: Brandner et al. (1996) have found an X-ray detection bias for binaries in Scorpius-Centaurus of 1.17 towards X-ray selected TTS, and Köhler et al. (1998) have found an detection bias of ROSAT discovered TTS of 1.20. Note that all these values are only rough estimates, because of different sensitivities in the different binary surveys.

3.3. Detection rates

In Tables 2 and 3 we present the results of the detection rate study, for the sample with and without EO-discovered TTS, respectively. The columns of both tables contain the object type, the number of TTS in each sample, the number of detected TTS, and the observed and expected detection rates. In some cases several TTS are found near (within 40″ of) a single X-ray source, so that it is not clear

Table 1. RASS detected and undetected TTS not included in the sample of N95 because of later discovery

Name	type & mult.	Ref.	cts	exp. [s]
LkHα 272	c	1	≤ 9	414
LkHα 273	c	1	≤ 9	414
IRAS 03577+3134	c	2	≤ 4	414
IRAS 03580+3135	bc	2	≤ 10	430
Kim 3-89	w	3	≤ 6	644
Haro 6-37	tc	4	≤ 8	462
RW Aur	tc	4	9 ± 4	452
NTTS 040012+2545	bw	5	≤ 6	329
LkCa 1	w	6	≤ 11	473
L1495 IRS	c	7	≤ 9	471
IRAS 04181+2654	bc	7	≤ 11	645
IRAS 04385+2550	c	7	≤ 7	465
IRAS 04108+2910	c	7	≤ 7	478
IRAS 04151+2512	c	7	≤ 8	517
IRAS 04171+2756	c	7	≤ 11	644
IRAS 04200+2759	c	7	≤ 9	649
IRAS 04216+2603	c	7	≤ 9	540
IRAS 04260+2642	c	7	≤ 9	467
IRAS 04301+2608	c	7	≤ 8	463
Kim 1-44	c	7	≤ 7	467
IRAS 04414+2506	c	7	≤ 6	462
HHJ 339	c	8	≤ 7	367
HHJ 430	bc	8	≤ 5	318
MHO-3	c	9	≤ 2	479
2MWJ0417248+163436	w	10	≤ 8	397
LH0416+14	c	11	≤ 8	426
LH0418+15	c	11	≤ 7	463
LH0419+15	c	11	≤ 7	463
2MWJ0428299+235848	c	10	≤ 3	462
MHO-9	w	9	≤ 8	414
MHO-4	c	9	≤ 5	408
MHO-5	c	9	≤ 6	411
MHO-6	c	9	≤ 8	412
MHO-7	w	9	≤ 8	412
LH0429+15	c	11	≤ 5	435
LH0429+17	c	11	≤ 5	399
MHO-8	c	9	≤ 9	459
2MWJ0438352+173634	c	10	≤ 2	425
CIDA-13	w	12	≤ 7	474
CIDA-14	c	12	≤ 6	462
IRAS 04429+1550	c	13	83 ± 10	463
DG Tau B	c	14	≤ 9	459
Kim 3-76	w	15	≤ 3	629
IRAS 04154+2823	c	9	≤ 4	637
CoKu Tau/1	c	14	≤ 18	643
CoKu Tau/2	c	14	≤ 9	408
St 34	c	14	≤ 8	448

Ref.: (1) Herbig & Bell (1988), (2) Kenyon et al. (1990), (3) Strom & Strom (1994), (4) Cohen & Kuhi (1979), (5) Walter et al. (1988), (6) Herbig et al. (1986), (7) Kenyon et al. (1994), (8) Oppenheimer et al. (1997), (9) Briceño et al. (1998), (10) Giziz et al. (1999), (11) Reid & Hawley (1999), (12) Briceño et al. (1999), (13) Torres et al. (1995), (14) Kenyon & Hartmann et al. (1995), (15) Briceño et al. (1993).

Table 2. Detection rates of TTS in the RASS for the sample including EO TTS. Expected detection rates for binaries are computed from observed detection rates of single cTTS and wTTS. In brackets: Without the stars from Table 4 (ambiguous in the RASS, but resolved with the HRI)

sub-sample	size		no. of det.		detection rate x		expected det. rates $1-(1-x)^2$	
all TTS	199⋆	(184)	59	(50)	30±4%	(27±4%)		
all cTTS	125	(114)	15	(9)	12±3%	(8±2%)		
all wTTS	76	(71)	45	(40)	59±9%	(56±9%)		
all single cTTS	92	(87)	8	(5)	9±3%	(6±3%)		
all single wTTS	43	(42)	19	(18)	44±10%	(43±10%)		
all binary cTTS	25	(19)	4	(1)	16±8%	(5±5%)	17±6%	(12±5%)
all binary wTTS	24	(21)	19	(17)	79±18%	(81±20%)	79±18%	(68±10%)
all triple cTTS	6		3		50±29%			
all triple wTTS	7	(5)	6	(4)	86±35%	(80±40%)		
all quadruple cTTS	2		0		0%			

⋆ DD/CZ Tau are not considered because none of them is detected with the HRI (see Table 4).

Table 3. Detection rates of TTS in the RASS for the sample without EO TTS. Expected detection rates for binaries are computed from observed detection rates of single cTTS and wTTS. In brackets: Without the stars from Table 4 (ambiguous in the RASS, but resolved with the HRI)

sub-sample	size		no. of det.		detection rate x		expected det. rates $1-(1-x)^2$	
all TTS	176⋆	(161)	40	(30)	23±4%	(19±3%)		
all cTTS	123	(115)	15	(8)	12±3%	(7±3%)		
all wTTS	51	(46)	25	(22)	49±10%	(48±11%)		
all single cTTS	92	(87)	8	(5)	9±3%	(6±3%)		
all single wTTS	20	(19)	10	(9)	50±16%	(47±16%)		
all binary cTTS	24	(19)	3	(1)	12±7%	(5±5%)	17±6%	(12±6%)
all binary wTTS	14	(11)	11	(9)	79±24%	(82±27%)	75±13%	(72±12%)
all triple cTTS	6		3		50±29%			
all triple wTTS	6	(4)	5	(3)	83±37%	(75±43%)		
all quadruple cTTS	2				0%			

⋆ DD/CZ Tau are not considered because none of them is detected with the HRI (see Table 4).

which TTS is the true optical counterpart. Because these stars were also observed and resolved with the HRI, the confusions could be cleared. This implies that the sources are not variable and did not change their nature during the time between the RASS and the HRI observation. For the case that this assumption does not hold we investigate the sample also without these ambiguous sources (numbers in brackets in Table 2).

As it can be seen from Tables 2 and 3, more wTTS than cTTS are detected, and the detection rate of binaries is higher than that of single TTS. The detection rates of binary cTTS and binary wTTS agree well with the expected values for cTTS-cTTS and wTTS-wTTS binaries, respectively. These results hold even if excluding the stars which could only be resolved by the HRI. The expected detection rate for mixed pairs is 49±10% (46±10%) which does not correspond to the observed detection rates of binary cTTS nor binary wTTS.

Regarding the detection rates of the stars which were not X-ray selected (Table 3) the expected values of cTTS-cTTS and wTTS-wTTS pairs again are consistent with the observed values of cTTS and wTTS binaries. For this sample we expect a detection rate of mixed cTTS-wTTS binaries of $54 \pm 16\%$ ($49 \pm 16\%$) which also does not correspond to the observed detection rates of cTTS nor wTTS binaries.

We now estimate the number of mixed pairs in our sample of cTTS binaries. The sample of binary cTTS consists of 25 stars, where in 6 cases the secondary is also known to be a cTTS. In the other 19 cTTS binaries the nature of the secondary is not known. Two of these were detected (XZ Tau and GK Tau), so that the detection rate of possibly mixed pairs is $11 \pm 7\%$. This is significantly below the expected detection rate for mixed pairs quoted in the previous paragraph. The number of mixed binaries in our sample is given by the expected detection rate divided

Table 4. HRI data of TTS binaries with ambiguous identifications in the RASS but resolved by the HRI

Designation	type*	α_{2000} [hh:mm:ss]	δ_{2000} [dd:′ ′:″ ″]	expo [s]	ML	cts [s]	$d\alpha$ [″]	$d\delta$ [′]	offax	HR
GK Tau	bc	04 33 34.5	24 21 07	20756	702	347 ± 19	0.03	2.0	0.39	0.45 ± 0.09
GI Tau	c	04 33 34.1	24 21 18	20762	394	222 ± 15	0.15	–3.0	0.37	≤ 0.72
V807 Tau	bc	04 33 06.6	+24 09 56	19341	257	218 ± 17	–0.01	6.3	12.60	0.50 ± 0.09
GH Tau	bc	04 33 06.2	+24 09 35	20899		≤ 252			12.95	
V773 Tau	bw	04 14 12.9	+28 12 12	3473	1385	318 ± 18	–0.02	–0.2	0.47	0.61 ± 0.02
FM Tau	c	04 14 13.5	+28 12 50	3473	34	113 ± 4	–0.06	–1.3	0.44	≥ 0.71
CW Tau	c	04 14 17.0	+28 10 59	3473		≤ 1			0.00	
DD Tau	bc	04 18 31.1	+28 16 30	11651		≤ 2			15.30	
CZ Tau	bw	04 18 31.6	+28 17 00	11651		≤ 64			15.30	
DH Tau	c	04 29 42.0	+26 32 48	7146	44	23 ± 5	0.0	0.0	0.25	≥ 0.81
DI Tau	bw	04 29 42.5	+26 32 50	7144	212	85 ± 10	–0.01	1.3	0.45	0.20 ± 0.02
HL Tau	c	04 31 38.4	+18 13 59	5749		≤ 3			0.18	
XZ Tau S & N	bc	04 31 40.0	+18 13 58	5102	210	65 ± 8	–0.02	1.7	0.42	0.47 ± 0.07
HP Tau	tw	04 35 53.1	+22 54 24	5551	49	27 ± 6	0.06	0.7	0.22	0.44 ± 0.08
CoKu HP Tau/G2	tw	04 35 54.4	+22 54 14	5553	450	144 ± 12	–0.02	0.6	0.54	0.71 ± 0.04
CoKu HP Tau/G3	tw	04 35 53.5	+22 54 10	6150		≤ 108			0.47	
Haro 6-28	bc	04 35 55.9	+22 54 36	6657		≤ 3			0.71	
LkHα 332/G1	tw	04 42 06.9	+25 23 04	15785	54	56 ± 8	–0.43	–1.3	0.28	0.27 ± 0.01
CoKu LkHα 332	tw	04 42 06.9	+25 23 11	18670		≤ 51			0.23	
LkHα 332/G2	w	04 42 05.5	+25 22 57	15775	968	343 ± 19	0.04	1.8	0.57	0.15 ± 0.02

$\star$ c: single cTTS, w: single wTTS, bc: binary cTTS, bw: binary wTTS, tw: triple wTTS.

by the observed detection rate, i.e. $4.5 \pm 2.3\%$ which gives 0.9 ± 0.3 mixed pairs among our sample.

We conclude that a binary TTS is almost always composed of two stars with the same nature: cTTS binaries consist of two cTTS, and wTTS binaries of two wTTS.

4. The HRI study of resolved binaries

In this part of the paper we study the X-ray emission of the HRI resolved wide TTS binaries. Our sample consists of cTTS and wTTS in Taurus with separation $\geq 5''$ corresponding to $\sim$700 AU at a distance of 140 ± 10 pc. The sample is compiled from Chen & Simon (1990), Simon et al. (1992), Leinert et al. (1993), Ghez et al. (1993, 1995, 1997a), Reipurth & Zinnecker (1993), Hartigan et al. (1994), Richichi et al. (1994), and Simon et al. (1995). There are a total number of 30 TTS in Taurus with separations larger than $5''$. Of those, 9 multiples have been observed by the HRI. Most of them by P. I. R. Neuhäuser and/or F. Walter with the purpose of resolving the pairs and investigate whether the primaries and the secondaries differ in their X-ray properties. The nature of the companion is known in 7 out of 9 cases: 6 are wTTS-wTTS and 1 is a cTTS-cTTS binary. Note that among the resolved systems no cTTS is coupled with a wTTS, in agreement with our result from Sect. 3 that most TTS binaries form pairs of equal type.

4.1. Data reduction

Source detection and identification was carried out with the EXSAS based on a maximum likelihood (ML) technique (Cruddace et al. 1988). We searched for offsets of the X-ray positions due to limitations in the ROSAT aspect determination by correlating Simbad and the Guide Star Catalog (GSC) with all detected X-ray sources. For the shifted HRI-fields a bore sight correction was applied (see Table 4.2). For all detected X-ray sources, we searched for optical counterparts among our sample of TTS. In Table 4.2 we list all detected and resolved multiple TTS. Given are designation and T Tauri type (c: cTTS, w: wTTS, ?: nature c or w unknown), spectral type, V magnitude, optical position (J2000), exposure time, maximum likelihood (ML) for detection, background-subtracted X-ray counts, distance between the optical and the X-ray position, off-axis angle, hardness ratio (HR, see Sect. 4.5), X-ray luminosity, X-ray over bolometric luminosity, projected rotational velocity, rotation period, and separation.

Unresolved companions with separation $<5''$ are listed with their primary star as one object. For binaries which are not properly resolved the closest optical object is considered to be the counterpart (see Fig. 1).

The extraction of the X-ray counts in close binaries was performed using the standard extraction radius of 2.5 FWHM of the point spread function. For the two binaries which are not properly resolved by the HRI (see Fig. 1, GI/GK Tau, SAO 76411 A & B) the source radius was decreased in order to avoid contamination of the count rates due to the companion star. With an extraction radius half the distance between the centers of the two sources, we determined the flux ratio. Then, using the total flux from the multiple system, we scaled the individual fluxes of the companions accordingly. The upper limits of the undetected companions contain all counts (including

Table 5. TTS sample used in N95 to evaluate the RASS detection rates. We have revised the list concerning the TTS nature (c or w) and the multiplicity. In our study (see Sect. 3.3) we additionally include TTS discovered since then. They are listed separately in Table 1

	detected	**undetected**
single cTTS	FM Tau, BP Tau, AA Tau, DN Tau, DG Tau, DH Tau, GI Tau	L 1489 IRS, CW Tau, HL Tau, FN Tau, FP Tau, IRAS 04108+2803 B, CX Tau, Briceño 1, CY Tau, Strom Anon 13, IRAS 04166+2706, J2-157 IRAS 04158+2805, IRAS 04181+2655, FT Tau, IRAS 04169+2702, IRAS 04187+1927, DE Tau, RY Tau, IRAS 04239+2436, HH 31 IRS 2, IQ Tau, IRAS 04264+2433, Haro 6-13, L1536 IRS, DL Tau, IRAS 04303+2240, DM Tau, CI Tau, HO Tau, IRAS 04325+2402, JH 112, DO Tau, LkCa 15, IRAS 04361+2547, GM Tau, IRAS 04365+2535, IRAS 04368+2557, DR Tau IRAS 04369+2539, DP Tau, IRAS 04381+2540, Briceño 7, DS Tau, GO Tau, IRAS 04489+3042, GM Aur, Briceño 8, IRAS 05023+2527, Briceño 11, Briceño 12
single wTTS	NTTS 032641+2420, SAO 76428, Anon 1, Hubble 4, Lick 6, NTTS 041559+1716, HD 283572, IP Tau, NTTS 042417+1744, Lick 3, JH 56, NTTS 042835+1700, SU Aur, V827 Tau, V830 Tau, LkCa 14, LkCa 19, V836 Tau, Briceño 10, CoKu LkH$_\alpha$ 332/G2	NTTS 040234+2143, Briceño 2, LkCa 4, LkCa 5, IRAS 04147+2822, NTTS 041529+1652, LkCa 21, J 4423, J 507, L 1551/IRS 5, J 665, J2-2041, JH 108, NTTS 043124+1824, NTTS 043220+1815, JH 223, CoKu Tau/4
binary cTTS	XZ Tau, V710 Tau, V807 Tau, GK Tau	IRAS 04113+2758, FO Tau, FQ Tau, FW Tau, IRAS 04181+2654, DF Tau, GV Tau, DK Tau, ZZ Tau A (R), HK Tau, FY/FZ Tau, IS Tau, HN Tau, Haro 6-28, GN Tau, UY Aur, DQ Tau, GH Tau
binary wTTS	NTTS 034903+2431, NTTS 035135+2528, SAO 76411, NTTS 040142+2150, LkCa 3, V819 Tau, LkCa 7, J 4872, L1551-51, V826 Tau, V928 Tau, IT Tau, FF Tau, NTTS 043230+1746, CoKu Tau/3, VY Tau, IW Tau, NTTS 045251+3016, DI Tau	NTTS 035120+3154, NTTS 040012+2545, FX Tau, V927 Tau
triple cTTS	T Tau, UZ Tau	FS Tau, PP 13
triple wTTS	NTTS 040047+2603, UX Tau, HP Tau, V410 Tau, CoKu LkH$_\alpha$ 332, V773 Tau	HV Tau
quadruple cTTS		FV Tau, GG Tau

background) extracted at the position of the optical counterpart in a radius of 2.5 FWHM at that off-axis angle.

4.2. The nature of the secondaries

In principle the visual multiples studied can be physically bound or chance projections. Old background objects should show less X-ray emission than young TTS in Taurus or no X-rays at all. Some of the secondaries are clearly detected in X-rays, so that they are possibly young, increasing the probability that the pairs are bound. This conclusion can be drawn for: GI/GK Tau, NTTS 0400147+2603 E & W, HP Tau & HP Tau/G2 and SAO 76411 A & B. The nature of SAO 76411 B is not known. Its X-ray emission could indicate that it is a wTTS, because wTTS in Taurus are X-ray brighter than cTTS. If it would be a cTTS one should see signs of its H$_\alpha$-emission in the spectra. For UX Tau A & B and NTTS 0404142+2150 NE & SW the X-ray sources are elongated along the optical position which might be a hint that both stars emit X-rays. UX Tau B is 3 mag fainter in the optical than UX Tau A. V819 Tau/c whose T Tauri type is not known, is clearly undetected in X-rays. This seems to indicate that V819 Tau/c is an old background object. We note that very recently both 2000 and White & Ghez (in prep.) found direct evidence that V819 Tau/c is not a young object and therefore indeed not a companion to the TTS V819 Tau.

4.3. X-ray luminosity and spectral hardness

In this section we compare the X-ray luminosity L_X of the primary and the secondary in our sample stars. Only systems which are clearly resolved are used for this part of the analysis. The component with brighter V magnitude and earlier spectral type is always regarded as the primary. Unresolved binaries of hierarchical triples are treated as one star. We do not include

Table 6. Properties of TTS binaries and multiples[⋆] in Taurus resolved by the ROSAT HRI

				V	α_{2000}	δ_{2000}		α	δ		L_X	L_{bol}	v	i		
					′ ′ ″	′ ″		″	′		$\frac{erg}{sec}$	$\frac{erg}{sec}$	$\frac{km}{s}$			″
201089/201623 Zinnecker, bc:								−1.	,	−1.	″					
			(a)		12 1		2 21	2	2	±1	2	. ± .	. ± . 2	(b)	1 (e)	(h) 2 (b)
			(a)		1 1		1 2 21 1	2	2	222 ± 1	1	≤ 2	.2 ± .	(b)	11 2 (e)	2 (g) 12 2 (c)
201058 Walter, bc:								1.1	,	−1.	″					
2	⋆⋆		(i)	2 1 1			2 1		21	±1	1 1	.11 ± . 1	. 2 ± .	(b)	≤1 (a)	2 (b)
2		⋆⋆	(i)	2 1 2			2 2 1		12	±	2	2 . ± .	2 . ± .	(b)		1 (b)
201617 Zinnecker																
			(a)	2 1 1			1 22	2	1	2 ±		22 . ± .	.21 ± .1	(b)	1 (e)	(h)
	2		(a)		11 1		22	12		1 ± 12	2	. 1 ± .	. ± .	(b)	1 (a)	1 2 (h) 2 (b)
			(a)		1		22	1	1	≤1			≤	(b)		(b)
201622 Zinnecker, bc:								−1.	,	−2. 2	″					
α	2 1		(b)	1 1 1		2	2 2		1	±	1 2	.2 ± . 1	.1 ± .	(b)		22 (j)
	α 2		(b)		1	2	2 2	11	1	≤ 1	2	≤2 1		(b)	1 1 (e)	(a)
201057/202029 Neuhäuser/Walter, bc:								− .	s,	−1.	″					
1	2 2	⋆⋆	(i)		12		2			1 ±		.2 ± .11	2 . ± .	(b)	2 (a)	(b)
1	2 2	⋆⋆	(i)		1		2	12	2	≤		≤2	2	(b)	≤1 (a)	(b)
202030/201053 Neuhäuser/Walter																
1 2 21		⋆⋆	(i)		1		21	22		11 ± 11	2 2 2	. ± .	. ± .	2 (b)	2 (a)	2 (b)
1 2 21		⋆⋆	(i)		1		21	2	2	≤ 111		≤	2 (b)		12 (a)	2 (b)
201838 Walter																
	11		(i)	1		2	22	12	12	1 2 1 2 ± 1		. ± .	2 . ± .	(k)	12 (d)	(a)
	11			1 1		2	22	12	1	±	1	.2 ± .	2 . ± .	(k)	≤ (a)	(a)
201619 Zinnecker																
			(a)	1			1 1	22		1 ± 11	1 1	. ± .	.2 ± .	(b)	2 (e)	2 (h) (b)
			(a)	2 1			1 1			≤ 11		≤		(b)	1 (e)	(b)
202156 Neuhäuser																
1			(a)		1 2	1 2 2	2 2 1			1 ± 1	1	. ± .	. 2 ± .	(f)	≤1 (a)	(g) 1 (c)
1				12.1	(l)	1 2	2 2 1			≤ 2	2	≤2	2	(b)	1	1 (c)

⋆ For all pointings ROSAT Observation Request Number and PI are given. A bore sight correction was applied to some fields indicated by bc and the offset.
⋆⋆ NTTS object. (a) Herbig & Bell (1988), (b) Hartigan et al. (1994), (c) Leinert et al. (1993), (d) Patterer et al. (1993), (e) Hartmann & Stauffer (1989), (f) Kenyon & Hartmann (1995), (g) Shevchenro et al. (1991), (h) Bouvier et al. (1993), (i) Walter et al. (1988), (j) Ghez et al. (1993), (k) derived using the photometry in (1988), (l) derived using the photometry in Leinert et al. (1993) assuming a bolometric correction of 2.

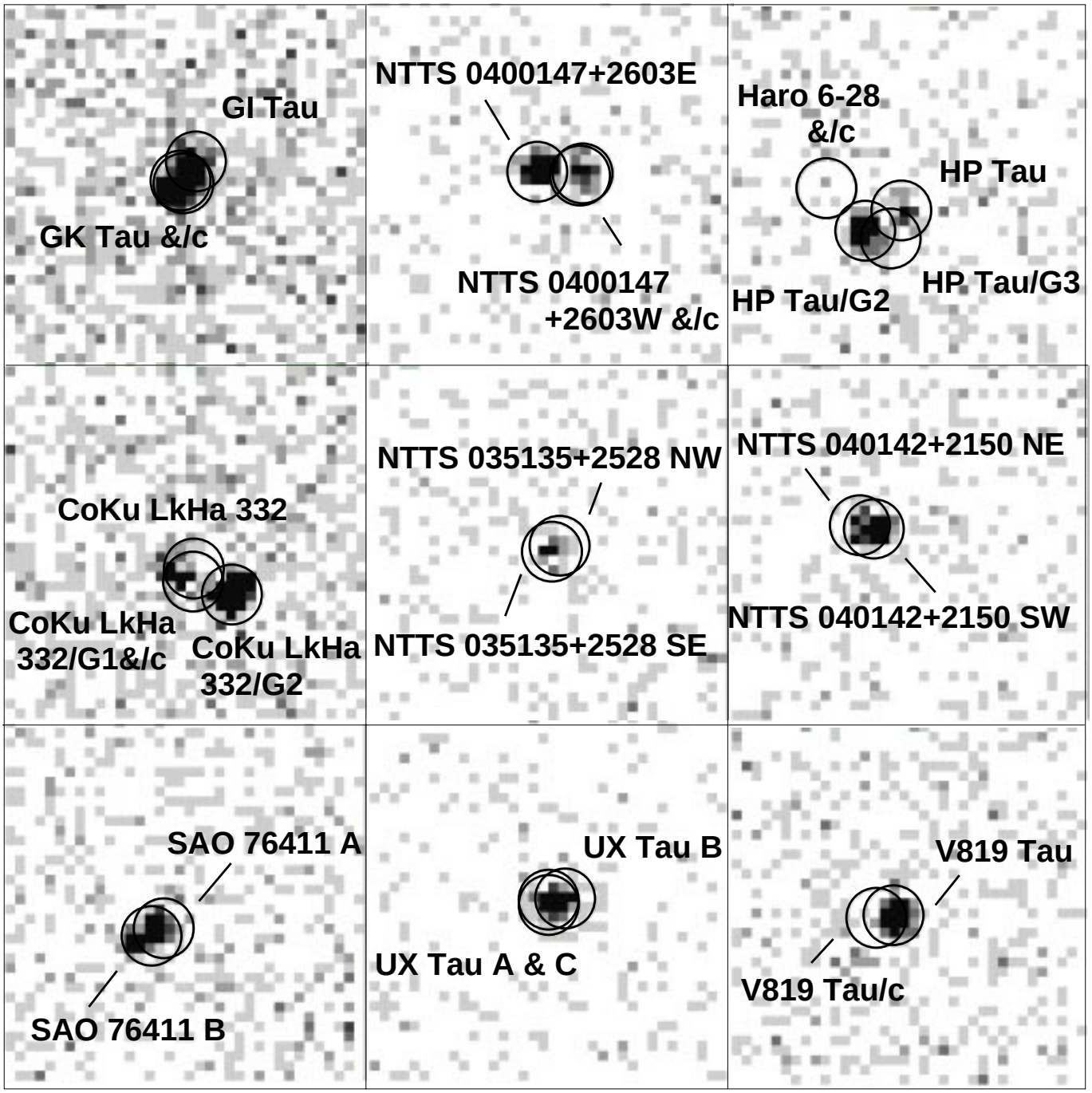

Fig. 1. ROSAT image of all multiple TTS in Taurus observed and resolved with the HRI. The HP Tau group (upper right) is a triple with two clearly detected and resolved X-ray sources, and the undetected component HP Tau/G3. The nearby binary Haro 6-28 is not detected. In the images of NTTS 0404142+2150 and UX Tau the X-ray source is slightly elongated along the positions of the optical counterparts. The X-ray counterpart of NTTS 035135+2528 is very faint and the separation of the binary ($6''$) is at the limit of the angular resolution of the HRI. In these cases we have assigned the X-ray emission to the closest optical counterpart (see Table 4.2)

NTTS 040142+2150 NE & SW because we cannot identify the primary by its V magnitude (considering the errors) or spectral type. Our estimate of the X-ray luminosities is based on a 1 keV Raymond-Smith model with solar metallicity (see N95). The corresponding X-ray flux $F_{\rm X}$ is computed with EXSAS using the column densities $N_{\rm H}$ listed by N95. The X-ray luminosity is derived from the measured flux $F_{\rm X}$ assuming a distance to Taurus of 140 ± 10 pc. The uncertainties of $L_{\rm X}$ originate from the uncertainties in count rate and distance.

To compare $L_{\rm X}$ of primaries and secondaries, we calculate the Kaplan-Meier estimator (KME) using the software package ASURV (Feigelson & Nelson 1985;

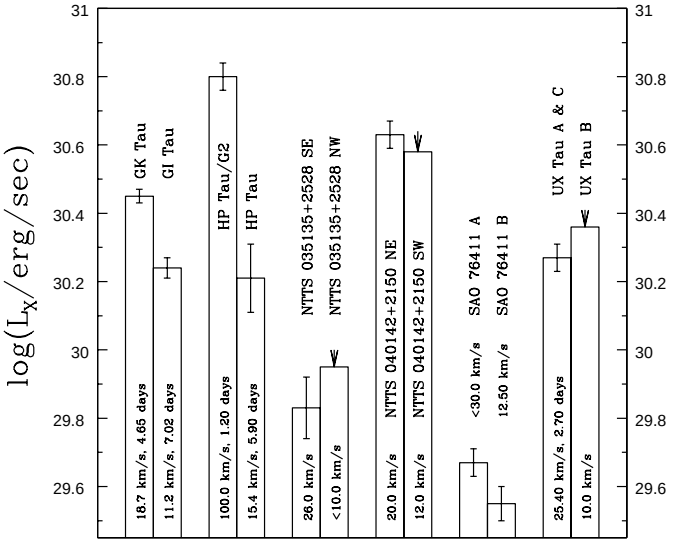

Fig. 2. Comparison of the X-ray luminosity within probably physically bound TTS. Upper limits are indicated by an arrow. Generally the faster rotating component emits more X-rays. In the case of NTTS 035135+2528 the pair could not clearly be resolved by the HRI and the upper limit for NTTS 035135+2528 NW might be to high

Isobe et al. 1986) which allows us to properly treat upper limits for undetected TTS.

All HRI data of resolved TTS multiples have been compiled and are listed in Table 6 together with relevant optical and rotational data. We obtain the following results (see Table 4.2 and Fig. 2):

- It is always the primary that emits more X-rays than the secondary in terms of L_X. This could be due to the fact that the primaries are also brighter in the optical and IR than the secondaries;
- In terms of L_X/L_{bol}, the primaries show (always) only slightly higher values than the secondaries. The reason for this is not obvious;
- The primaries emit always harder X-rays than the secondaries.

Interestingly, it is always the primary that rotates faster than the secondary, in the sample studied here, in terms of both rotational periods as well as projected rotational velocity $v \cdot \sin i$. Enhanced dynamo activity due to faster rotation may therefore explain the stronger and harder X-ray emission of primaries compared to the secondaries in our sample. For more details, X-ray luminosity functions, and Kaplan-Meier estimators see König et al. (2000).

4.4. Variability

As the primaries always rotate faster than the secondaries, we expect stronger activity in the primaries, if an α-Ω-dynamo is at work. As mentioned above this should include enhanced frequency of small flares. Because X-ray emission becomes harder during flares (Preibisch et al. 1993), a star with many small flares should appear harder. This may explain why the primaries are harder in X-rays than secondaries. Most of these flares may well be too short and too weak to be noticed in the ROSAT data.

We have generated light curves with binsize of 400 s. Shorter binsizes could introduce artificial variations due to the satellite's wobble motion. In two cases (GK Tau and SAO 76411 A) we found variability on the 2σ to 3σ level on the primary, but no variation on the secondary. Due to large data gaps, we can not make any statement about the rise and the decay of the count rate.

5. Summary

The RASS provides a spatially unbiased flux-limited sample of TTS well suited for a study of the detection rates of different subsamples of TTS.

In the Taurus region the detection rate of single wTTS is significantly higher than that of single cTTS. From the observed detection rates of cTTS and wTTS binaries in comparison with the expected detection rates for cTTS-cTTS and wTTS-wTTS binaries it follows that if one star of the physically bound multiple is identified as cTTS or wTTS, all other components have the same nature. Mixed pairs are very rare (0.9 ± 0.3 in a sample of 19 cTTS where the nature of the secondary is not known). Otherwise the detection rate of binary cTTS would be much higher than the expected value, and for wTTS binaries it would be much lower. The result does not depend on including the EO discovered TTS. The detection bias concerning binary TTS in EO observations is 1.18 ± 0.5.

In the second part of this paper we have studied the X-ray emission of wide TTS binaries, which were observed and resolvable by the ROSAT HRI. In this part of the analysis we have taken benefit from the fact that binary stars represent co-eval pairs which have evolved under the same conditions, and thus are represented by the same distance and metallicity. Furthermore, the detection of both components of wider pairs in X-rays is an indication that both stars are young, and therefore have evolved under similar conditions at the same time.

In particular we have compared the X-ray emission of primary and secondary in resolved binaries to unveal influences of bolometric luminosity and rotation.

Primaries are more X-ray luminous than secondaries. The X-ray data of resolved multiple TTS shows that the X-ray luminosity over bolometric luminosity ratios of the sample of primaries is indistinguishable from the sample of secondaries but for all primaries it is slightly higher. This leads to the conclusion that the level of X-rays emitted is governed by the luminosity in the optical and IR. However, the faster rotating component always emits more X-rays than the slower rotating component. This is consistent with the general notion that the X-rays result from an α-Ω-dynamo. The stronger X-ray luminosity found in primaries compared to secondaries could, therefore, be due to higher bolometric luminosity and/or faster rotation of the primaries. To distinguish between these two

possibilities one should look for binaries where the secondary is the faster rotating component.

We find that the faster rotating star always emits harder X-rays. This is not unexpected in terms of dynamo models where faster rotating stars should produce more (small) flares, and flares be associated with hotter plasma, and thus harder spectra. This interpretation is supported by variability found in two primaries but in none of the secondaries. Further observations with higher angular resolution than achievable with ROSAT (5″) would be useful to confirm this result on a larger sample.

Acknowledgements. We would like to thank M. Sterzik, R. Köhler, W. Brandner and R. White for fruitful discussions and F. Walter, H. Zinnecker and F. Damiani, the PI's of some HRI pointings evaluated here. This research of made use of the Simbad data base, operated at CDS, Strasbourg, France. ROSAT is supported by the German government (BMBF/DLR) and the Max-Planck-Society. R. N. wishes to acknowledge financial support from the Bundesministerium für Bildung und Forschung through the Deutsche Zentrum für Luft- und Raumfahrt e.V. (DLR) under grant number 50 OR 0003.

References

Bouvier, J. 1990, AJ, 99, 946
Bouvier, J., Cabrit, S., Fernández, E. L., Martín, E. L., & Matthews, J. M. 1993, A&A, 272, 176
Brandner, W., Alcalá, J. M., Kunkel, M., Moneti, A., & Zinnecker, H. 1996, A&A, 307, 121
Brandner, W., & Zinnecker, H. 1997, A&A, 321, 220
Briceño, C., Calvet, N., Gomez, M., et al. 1993, PASP, 105, 686
Briceño, C., Hartmann, L., Stauffer, J., & Martín, E. 1998, AJ, 115, 2074
Briceño, C., Calvet, N., Kenyon, S., & Hartmann, L. 1999, AJ, 118, 1354
Chen, W. P., & Simon, M. 1990, AJ, 357, 224
Cohen, M., & Kuhi, L. V. 1979, ApJS, 41, 743
Cruddace, R. G., Hasinger, G. R., & Schmitt, J. H. M. M. 1988, The Application of a maximum likelihood analysis to detection of sources in the ROSAT data, in ESO Conference and Workshop Proc. 28, Astronomy from large databases, F. Murtagh, & A. Heck Garching, 177
David, L. P., Harnden, F. R., Kearns, K. E., et al. 1999, The ROSAT High Resolution Imager (HRI) Calibration Report
Duchêne, G. 1999, A&A, 341, 547
Elias, J. H. 1978, ApJ, 224, 857
Feigelson, E. D., & DeCampli, W. M. 1981, ApJ, 243, L89
Feigelson, E. D., & Nelson, P. I. 1985, ApJ, 293, 192
Feigelson, E. D., Casanova S., Montmerle, T., & Guibert, J. 1993, ApJ, 416, 623
Feigelson, E. D., & Montmerle, T. 1999, ARA&A, 37, 636
Gagné, M., Caillault, J.-P., & Stauffer, J. R. 1995, ApJ, 445, 280
Ghez, A. M., Neugebauer, G., & Matthews, K. 1993, AJ, 106, 2005
Ghez, A. M., Weinberger, A. J., Neugebauer, G., Matthews, K., & McCarthy, D. W. 1995, AJ, 110, 753
Ghez, A. M., McCarthy, D. W., Patience, J. L., & Beck, T. L. 1997a, ApJ, 481, 378
Ghez, A. M., White, R. J., & Simon, M. 1997b, ApJ, 490, 353
Gizis, J. E., & Reid, I. N. 1999, AJ, 117, 508
Grosso, N., Montmerle, T., Bontemps, S., André, P., & Feigelson, E. D. 2000, A&A, 359, 113
Hartigan, P., Strom, K. M., & Strom, S. E. 1994, ApJ, 427, 961
Hartmann, L., & Stauffer, J. R. 1989, AJ, 97, 873
Herbig, G. H., Vrba, F. J., & Rydgren, A. E. 1986, AJ, 91, 575
Herbig, G. H., & Bell, K. R. 1988, Lick Obs. Bulletin, 1111
Isobe, T., Feigelson, E. D., & Nelson, P. I. 1986, ApJ, 306, 490
Kenyon, S. J., Hartmann, L. W., Strom, K. M., & Strom, S. E. 1990, AJ, 99, 869
Kenyon, S. J., Dobrzycka, D., & Hartmann, L. W. 1994, AJ, 108, 1872
Kenyon, S. J., & Hartmann, L. W. 1995, ApJS, 101, 117
Köhler, R., & Leinert, Ch. 1998, A&A, 331, 977
König, B., Neuhäuser, R., & Stelzer, B. 2000, IAUS, 200, 91
Koresko, C. D. 2000, ApJ, 531, L147
Leinert, Ch., Zinnecker, H., Weitzel, N., et al. 1993, A&A, 278, 129
Magazzu, A., Martin, E. L., Sterzik, M. F., et al. 1997, A&A, 124, 449
Mathieu, R. D., Stassun, K., Basri, G., et al. 1997, AJ, 113, 1841
Neuhäuser, R., Sterzik, M. F., Schmitt, J. H. M. M., Wichmann, R., & Krautter, J. 1995a, A&A, 295L, 5
Neuhäuser, R., Sterzik, M. F., Schmitt, J. H. M. M., Wichmann, R., & Krautter, J. 1995b, A&A, 297, 391 (N95)
Neuhäuser, R. 1997, Science, 276, 1363
Oppenheimer, B. R., Basri, G., Nakajima, T., & Kulkarni, S. R. 1997, AJ, 113, 296
Patterer, R. J., Ramsey, L., Huenemoerder, D. P., & Welty, A. D. 1993, AJ, 105, 1519
Pfeffermann, E., Briel, U., Hippmann, H., et al. 1988, The focal plane instrumentation of the ROSAT telescope, in Proc. SPIE 733, 519
Prato, L., & Simon, M. 1997, ApJ, 474, 455
Preibisch, T., Zinnecker, H., & Schmitt, J. H. M. M. 1993, A&A, 279, L33
Reid, I. N., & Hawley, S. L. 1999, AJ, 117, 343
Reipurth, B., & Zinnecker, H. 1993, A&A, 278, 81
Richichi, A., Calamai, G., & Leinert, Ch. 1994, A&A, 286, 829
Shevchenro, V. S., Grankin, R. N., Ibragimov, M. A., et al. 1991, IBVS, 3652
Simon, M., Chen, W. P., Howell, R. R., Benson, J. A., & Slowik, D. 1992, ApJ, 384, 212
Simon, M., Ghez, A. M., Leinert, Ch., et al. 1995, ApJ, 443, 625
Stelzer, B., & Neuhäuser, R. 2000, A&A, submitted
Strom, K. M., & Strom, S. E. 1994, ApJ, 424, 237
Torres, C. A. O., Quast, G., de la Reza, R., Gregorio-Hetem, J., & Lépine, J. R. D. 1995, AJ, 109, 2146
Trümper, J. 1983, Adv. Space Res., 2, 241
Walter, F. M., Brown, A., Mathieu, R. D., Myers, P. C., & Vrba, F. J. 1988, AJ, 96, 297
Wichmann, R., Schmitt, J. H. M. M., Neuhäuser, R., et al. 1996, A&A, 312, 439
Wichmann, R., Bastian, U., Krautter, J., Jankovics, I., & Ruciński, S. M. 1998, MNRAS, 301, L39
Woitas, J., Leinert, Ch., & Köhler, R. 2000, A&A, submitted
Zimmermann, H. U., Boese, G., Becker, W., et al. 1998, EXSAS Users's Guide, MPE Report 257, ROSAT Scientific Data Center, Garching